Supplement of

Aerosol emission factors from traditional biomass cookstoves in India: Insights from field measurements

Apoorva Pandey et al.

Correspondence to: Rajan K. Chakrabarty (chakrabarty@wustl.edu) and Apoorva Pandey (apoorva@wustl.edu)

Kitchen layout

The test kitchen was located on second floor of a house. It had one window located on the front wall, a U-shaped mud stove was fixed to this wall. The only door to the room was left fully open during all burns. All real-time instruments were placed in the back of the room, their inlets connected, via conductive tubing, to an eight-armed steel probe. Two Minivol samplers collected $PM_{2.5}$ samples on Teflon and quartz filters.

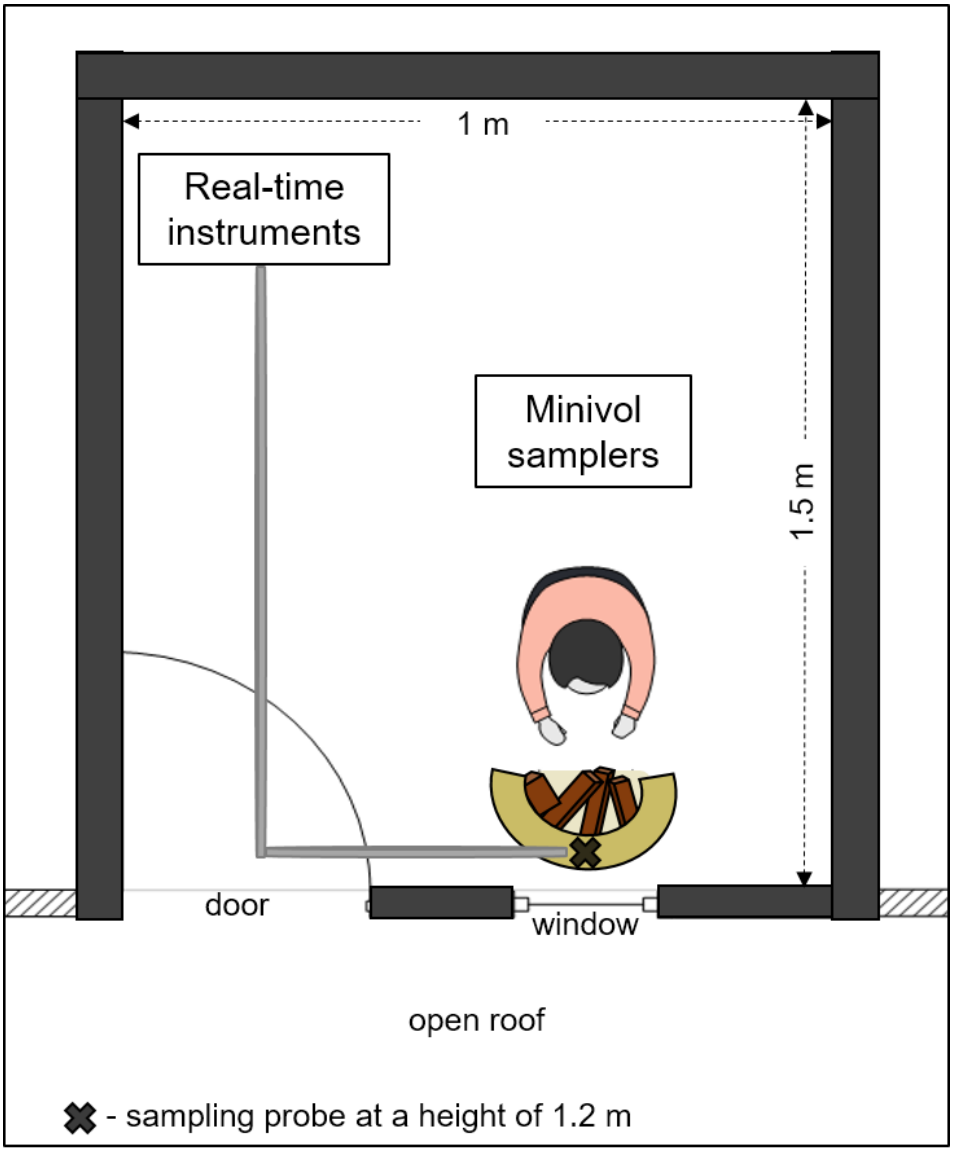

Figure S1: Schematic layout (top-view) of the kitchen

Wireless sensor data

Measurements from Sharp GP2Y sensors attached to the sampling probe (Sensor 1) and to the Minivol sampler (Sensor 2), from day 9 of the study, are shown in Figure S1. These sensors include an infrared emitting diode, the emission from which is scattered by the particles, and a phototransistor converts the scattered light to a voltage output proportional to the PM concentration.

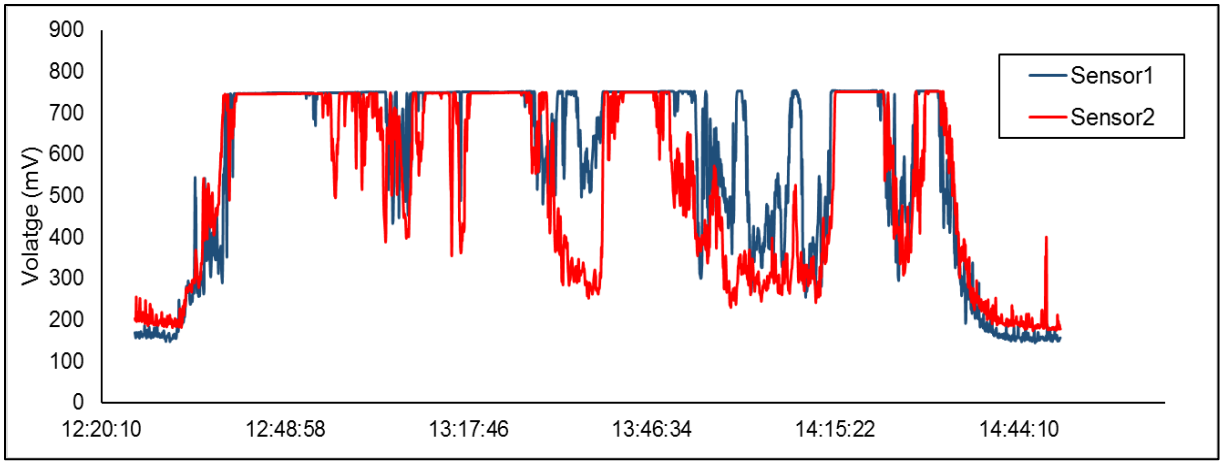

Figure S2: Raw signals from the PM sensors located at the sampling probe (Sensor1) and the Minivol $PM_{2.5}$ sampler (Sensor2).

The saturation voltage for the sensors is close to 750 mV, discarding all values higher than 750 mV, regression analysis of the remaining points yields a slope of 0.96. However, if the saturation threshold was set at 745 mV, the slope changed to 0.89. This is probably because saturation behavior for these sensors is a soft-limit saturation, such that the input-response relationship becomes non-linear at some voltage lower than the final limiting value of 750 mV. If measurements from this non-linear region are included, the linear regression analysis would give erroneous results. Therefore, we systematically reduced the threshold values until we observed negligible change in the regression slope. Finally, we discarded the data points where either of the sensors had readings above the linearity threshold (720 mV). About 60% of all data points were used, and a slope of 0.63 (R^2=0.65) was obtained. Therefore, the concentration measured by the Minivol sampler was adjusted upwards by a factor of 1.6 (=1/0.63).

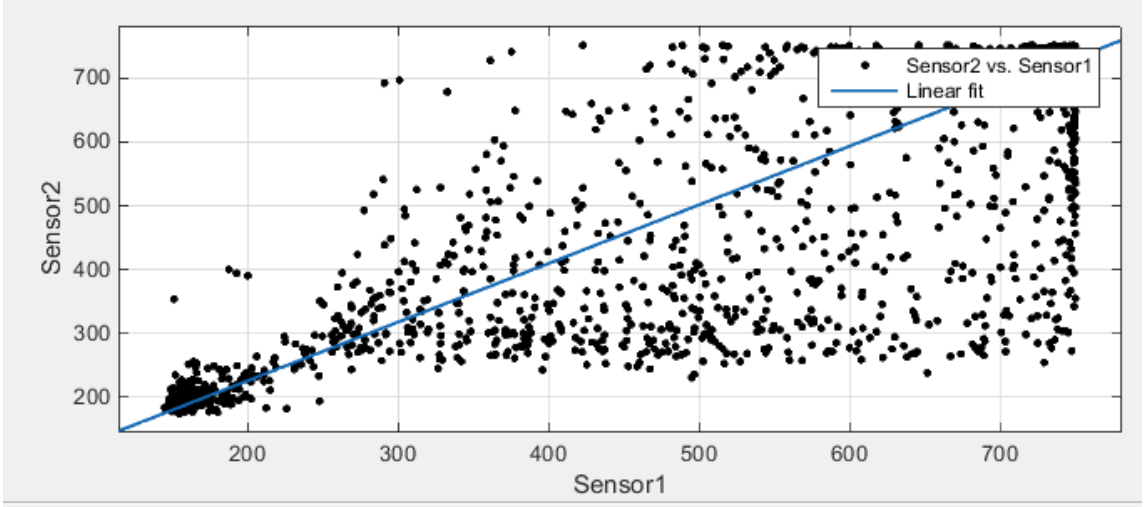

Figure S3: Scatter plot of measurements from Sensor1 and Sensor 2. Linear regression provided a slope of 0.63, with an R^2 of 0.65.

Real-time measurements

A sample plot of real-time particle and gas concentration profiles from day 9 of the study. Please note that the Sidepak instrument does not measure actual particle mass concentration, but instead measures light scattering at 670 nm wavelength and provides an equivalent concentration of Arizona Test Dust that would produce the same magnitude of light scattering.

Over a period of two hours, Sidepak PM measurements and CO concentration (solid in panel B) fluctauated every few minutes. Sidepak was saturated at an equivalent concentration of 20 µg/m3, giving the appearance of a steady state. Re-fueling typically caused a sudden change in particulate and CO emissions.

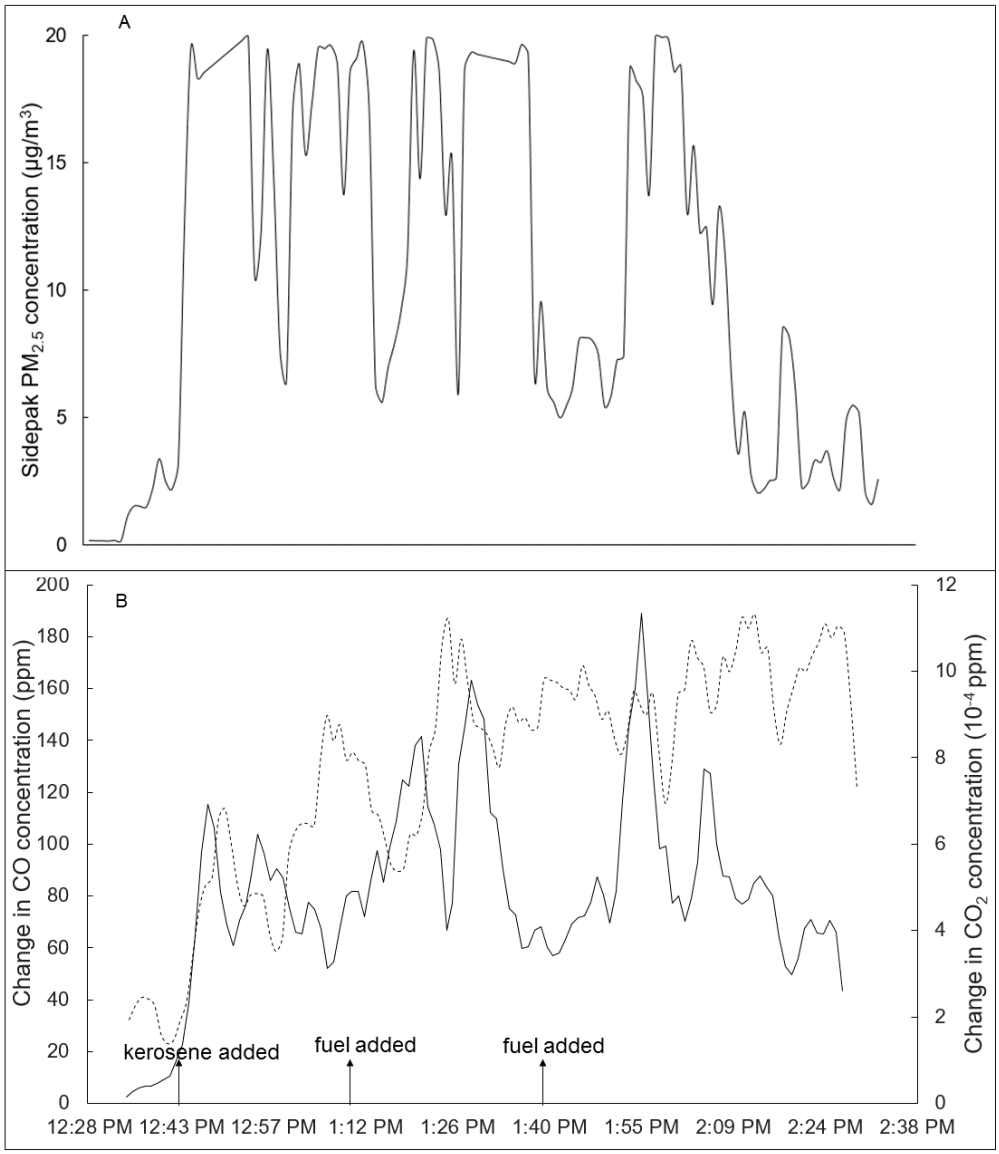

Figure S4: Real-time measurements of (A) Sidepak $PM_{2.5}$ mass concentrations in µg/m^3, and (B) CO concentrations (solid) in and CO_2 concentration (dashed), both in ppm.

Carbon Monoxide (CO) emission factors

Emission factors of CO were calculated using the equation below:

$$EF_{CO} = CMF_{fuel} \frac{C_{Co}}{\Delta C_{CO_2}\left(\frac{M_C}{M_{CO_2}}\right) + \Delta C_{CO}\left(\frac{M_C}{M_{CO}}\right)}$$

where EF_{CO} is the CO emission factor (g of CO released per kg of fuel burnt), CMF_{fuel} is the carbon mass fraction of the fuel, which ranged from 33% to 50% for the tested fuels. C_{CO} is the concentration of CO in g m^{-3}. ΔC_{CO2} and ΔC_{CO} are the concentrations above ambient levels of CO_2 and CO in g $m^{-3,}$ respectively. M_C, M_{CO2}, and M_{CO} are the atomic or molecular weights of C, CO_2, and CO in g $mole^{-1}$.

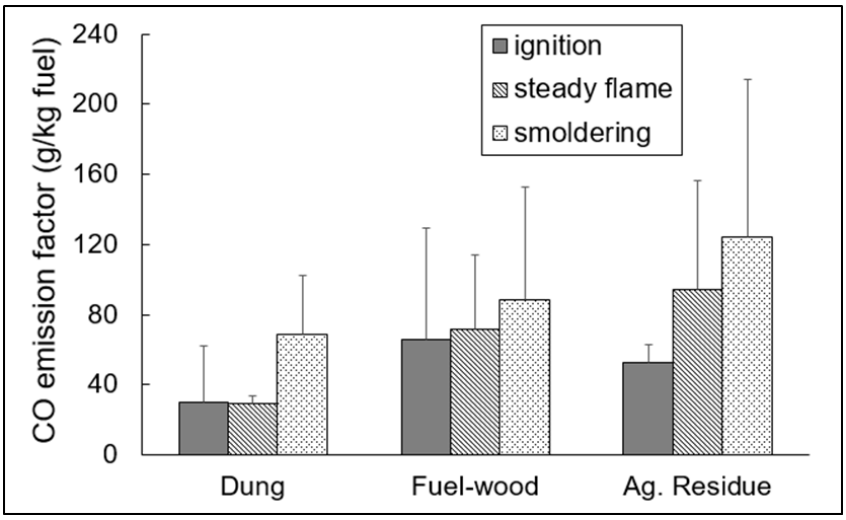

Figure S5: Fuel-wise average values of CO emission factors, categorized by observed combustion phases. One-sided error bars are shown to denote one standard deviation from the mean.

Both CO and $PM_{2.5}$ are products of incomplete combustion are their mass emission rates measured during lab cookstove tests are found to correlate (Roden et al., 2009). In this study, no correlation was observed between the estimated CO emission factors and corresponding $PM_{2.5}$ emission factors. Further, we plotted modified combustion efficiencies (MCE), calculated as the ratio of CO_2 concentration to $CO+CO_2$ concentration, against OC-to-EC ratios. MCE is typically treated as an identifier of combustion phase, with values greater than 0.9 associated with (Reid et al., 2005; Zhang et al., 2008). We found estimated MCE values above 0.9 for roughly 90% of all run time, even when no flaming phase was visibly observed. They showed no correlation with OC-to-EC ratios.

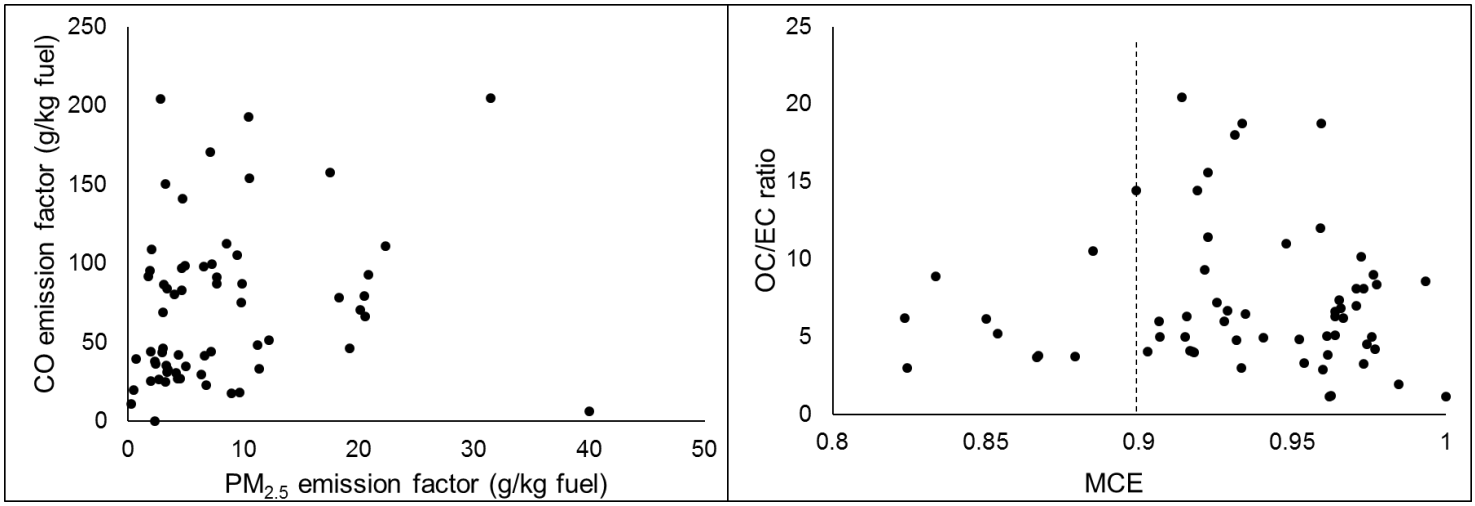

Figure S6: Comparisons of (a) CO vs $PM_{2.5}$, EFs and (b) OC/EC ratios vs modified combustion efficiency (MCE) values.

References

Reid, J., Koppmann, R., Eck, T. and Eleuterio, D. (2005). A review of biomass burning emissions part II: intensive physical properties of biomass burning particles. *Atmospheric Chemistry and Physics*, 5, 799-825.

Roden, C. A., Bond, T. C., Conway, S., Pinel, A. B. O., MacCarty, N. and Still, D. (2009). Laboratory and field investigations of particulate and carbon monoxide emissions from traditional and improved cookstoves. *Atmospheric Environment,* 43, 1170-1181.

Zhang, H., Ye, X., Cheng, T., Chen, J., Yang, X., Wang, L. and Zhang, R. (2008). A laboratory study of agricultural crop residue combustion in China: emission factors and emission inventory. *Atmospheric Environment,* 42, 8432-8441.